Supporting Information Available for

# Synthesis, Reaction, and Optical Properties of Cyclic Oligomers bearing 9,10-Diphenylanthracene Based on an Aromatic Tertiary Amide Unit

Ryohei Yamakado,[a] Shin-ichi Matsuoka,[a] Masato Suzuki,[a] Daisuke Takeuchi,[b] Hyuma Masu,[c] Isao Azumaya,[d] and Koji Takagi[a]*

a Department of Materials Science and Engineering, Nagoya Institute of Technology Gokiso-cho, Showa-ku, Nagoya 466-8555, Japan

b Chemical Resources Laboratory, Tokyo Institute of Technology, 4259 Nagatsuta-cho, Midori-ku, Yokohama 226-8503, Japan

c Chemical Analysis Center, Chiba University, 1-33 Yayoi-cho, Inage-ku, Chiba 263-8522, Japan

d Faculty of Pharmaceutical Sciences, Toho University, 2-2-1 Miyama, Funabashi, Chiba 274-8510, Japan

Contents

| | |
|---|---|
| 1. Synthesis of **C3A´**, **C4A´**, and **2** | S2–S3 |
| 2. Copy of NMR spectra | S4–S13 |
| 3. GPC profiles | S14 |
| 4. MALDI-TOF MS | S15–S16 |
| 5. UV and fluorescence spectra | S17–S19 |

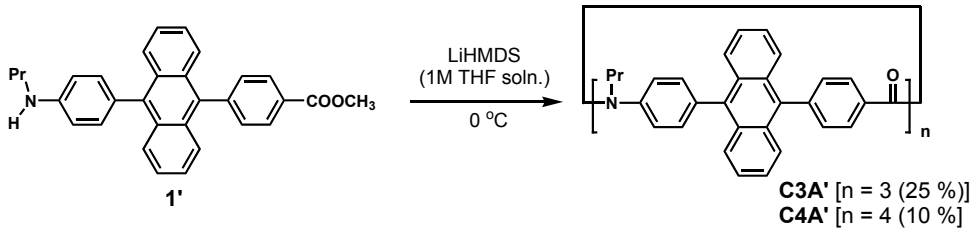


Scheme S1. Synthetic route to cyclic aromatic oligomers **C3A´** and **C4A´**.

**C3A´**

Yield, 25%. M.p. >300 ˚C. $^{1}$H NMR (δ, 600 MHz, ppm, $CDCl_3$) 7.64 (d, *J* = 8.0 Hz, 6H), 7.54 (d, *J* = 8.9 Hz, 6H), 7.47 (d, *J* = 8.9 Hz, 6H ), 7.41 (d, *J* = 8.2 Hz, 6H), 7.39–7.36 (12H), 6.94 (m, 6H), 6.89 (m, 6H), 4.21 (t, *J* = 7.8 Hz, 6H), 1.95 (m, 6H), 1.14 (t, *J* = 7.7 Hz, 9H). $^{13}$C NMR (δ, 150 MHz, ppm, $CDCl_3$) 170.5, 143.0, 140.7, 136.8, 136.2, 136.1, 135.9, 131.9, 130.6, 130.0, 129.9, 128.9, 128.1, 126.5, 126.1, 125.5, 125.2, 51.6, 21.2, 11.5.

**C4A´**

Yield 10%. M.p. >300 ˚C. $^{1}$H NMR (δ, 600 MHz, ppm, $CDCl_3$) 7.67 (d, *J* = 7.9 Hz, 6H), 7.60 (m, 6H), 7.57 (m, 6 H), 7.43 (d, *J* = 8.3 Hz, 6H), 7.41 (d, *J* = 8.3 Hz, 6H), 7.35 (d, *J* = 8.3 Hz, 6H), 7.15 (t, *J* = 7.0 Hz, 6H), 7.11 (t, *J* = 7.0 Hz, 6H), 4.17 (t, *J* = 7.4 Hz, 6H), 1.90 (m, 6H), 1.57 (m, 6H), 1.13 (t, *J* = 7.0 Hz, 9H). $^{13}$C NMR (δ, 150 MHz, ppm, $CDCl_3$) Not available due to low solubility.

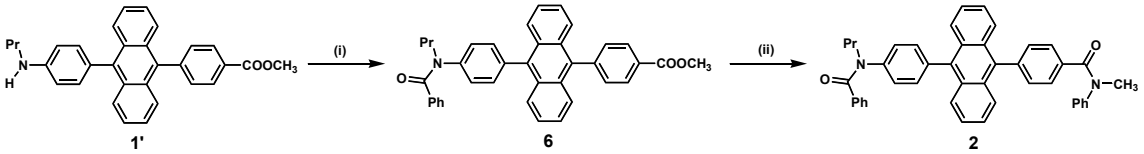


1' 6 2

Scheme S2. Synthetic route to model compound **2**. Condition and reagents: i) Benzoylchloride, Pyridine, THF, reflux; (ii) *N*-Methylaniline, LiHMDS (1 M THF soln.), THF, 0 ˚C.

**6**

Compound **1´** was prepared as **1**. To a solution of **1´** (222 mg/ 0.5 mmol) in pyridine (2 mL) and THF (2 mL) was added benzoylchloride (0.08 mL/ 0.6 mmol), and the system was heated to reflux overnight. The reaction mixture was poured into water, and an aqueous phase was extracted with DCM. The combined organic phase was washed with 1 M HCl. After drying over $MgSO_4$, solvents were removed by the rotary evaporator. The crude product was purified by column chromatography (ethyl acetate/DCM = 1/3) to obtain yellow powder (250 mg, 91%). M.p. 256–257 ˚C. $^1$H NMR (δ, 200 MHz, ppm, $CDCl_3$) 8.28 (d, $J$ = 8.6 Hz, 2H), 8.17 (d, $J$ = 8.0 Hz, 2H), 7.71–7.27 (17H), 4.10–3.90 (5H), 1.83 (m, 2H), 1.08 (t, $J$ = 7.0 Hz, 3H).

**2**

To a THF (5 mL) solution of **6** (250 mg/ 0.45 mmol) and *N*-methylaniline (0.08 mL/ 0.75 mmol) was added dropwise a 1.0 M THF solution of LiHMDS (1.0 mL), and the system was stirred for 10 h. After saturated aq. $NH_4Cl$ was added, an aqueous phase was extracted with DCM. A combined organic phase was dried over $MgSO_4$ and solvents were removed by the rotary evaporator. The resulted solid was recrystallized with $CHCl_3$/hexane to give yellow crystals (140 mg, 50%).

M.p. 329–330 ˚C. $^1$H NMR (δ, 200 MHz, ppm, $CDCl_3$) 7.53 (d, $J$ = 7.8 Hz, 2H), 7.51–7.46 (2H), 7.43 (d, $J$ = 7.8 Hz, 2H), 7.37–7.21 (d, $J$ = 7.9 Hz, 2H), 7.20 (d, $J$ = 8.6 Hz, 2H), 4.06 (d, $J$ = 6.1 Hz, 2H), 3.61 (s, 3H), 1.07 (t, $J$ = 6.1 Hz, 3H). $^{13}$C NMR (δ, 50 MHz, ppm, $CDCl_3$) 170.7, 170.4, 144.9, 140.2, 136.6, 136.2, 131.9, 130.7, 129.5, 129.1, 128.7, 128.1, 127.7, 127.1, 126.7, 125.1, 38.3, 30.3, 21.2, 11.5.

2. Copy of NMR spectra

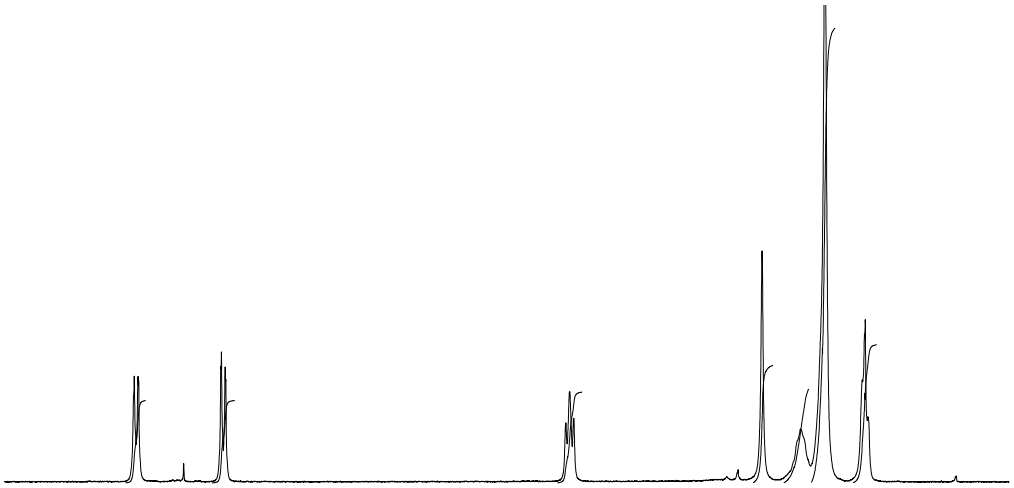

Figure S1. $^{1}H$ NMR spectrum of **3** in $CDCl_3$.

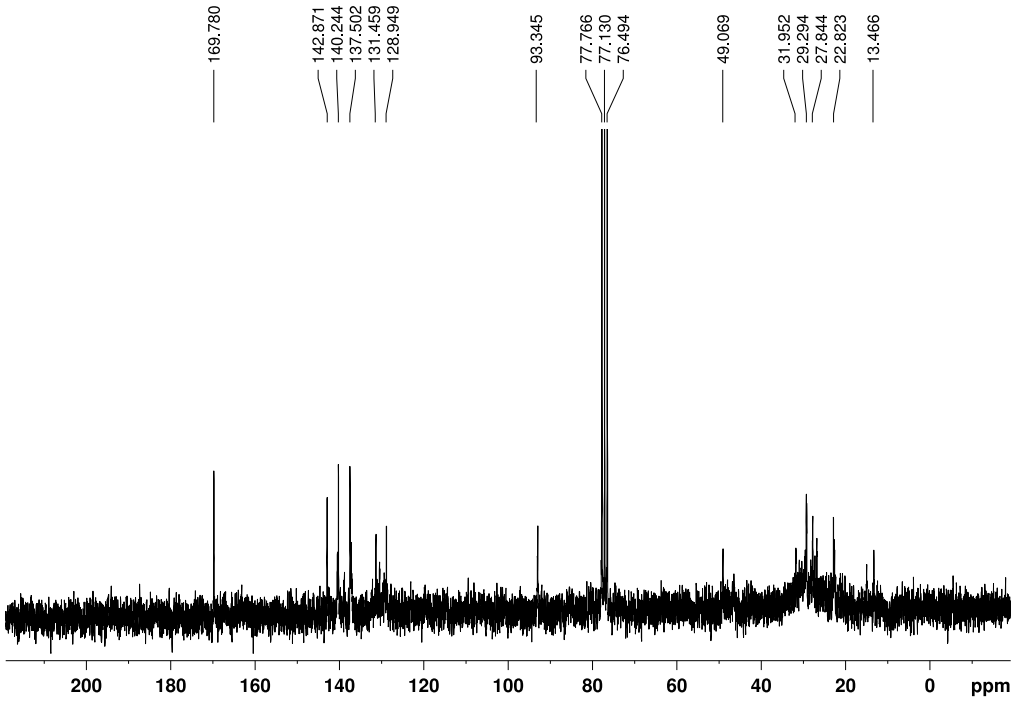


Figure S2. $^{13}C$ NMR spectrum of **3** in $CDCl_3$.

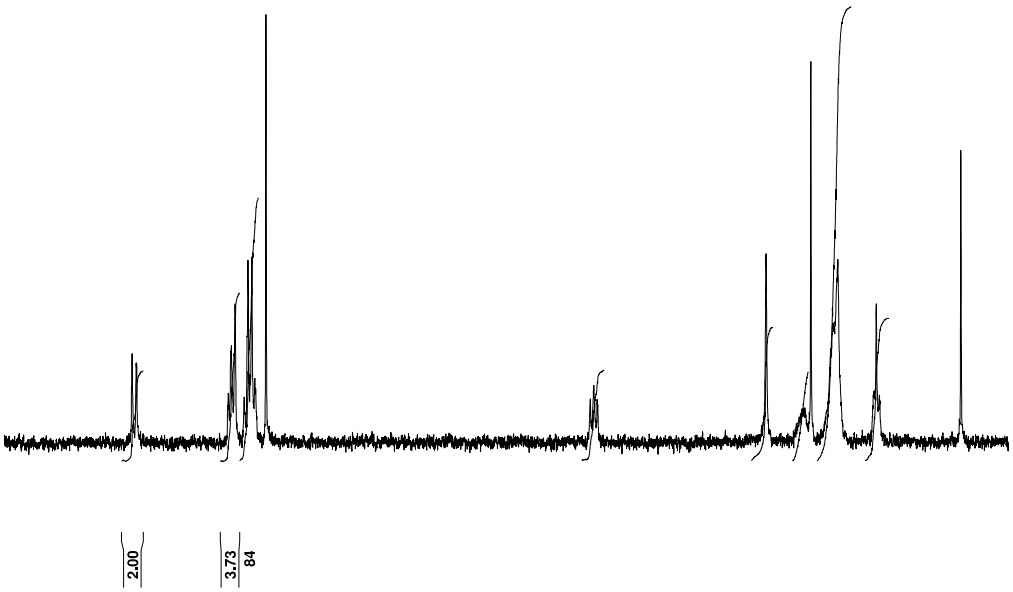


Figure S3. $^{1}$H NMR spectrum of **4** in $CDCl_3$.

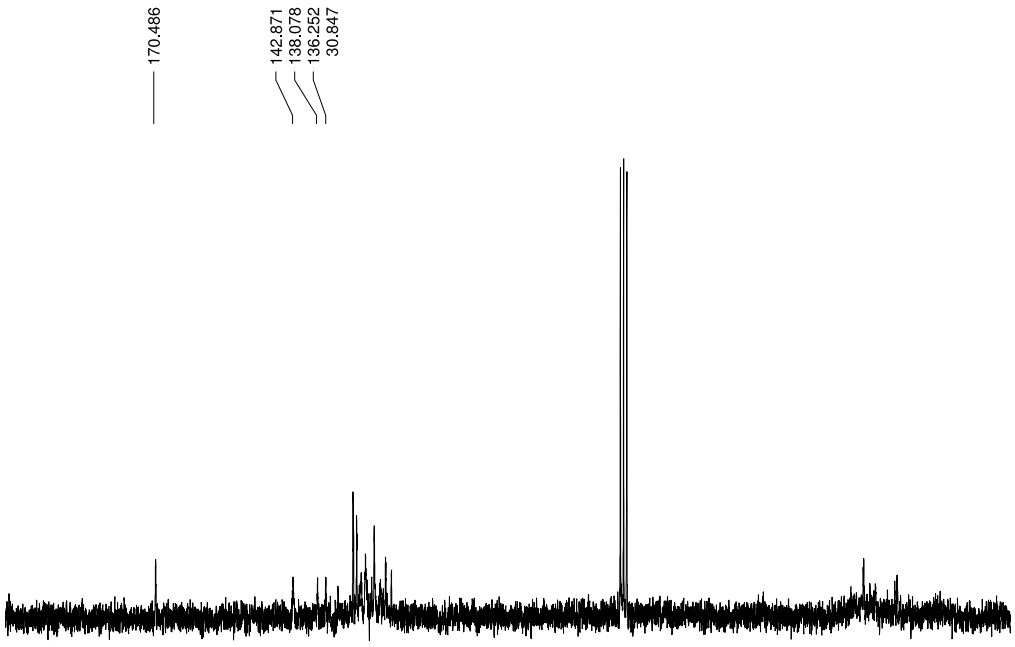


Figure S4. $^{13}$C NMR spectrum of **4** in $CDCl_3$.

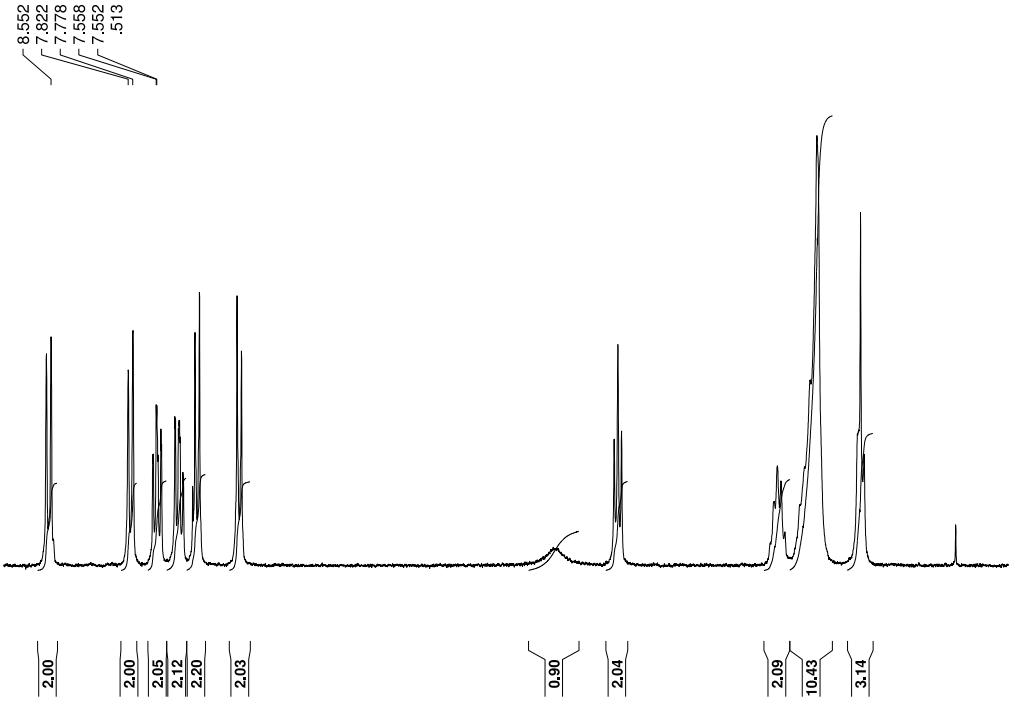


Figure S5. $^{1}$H NMR spectrum of **5** in $CDCl_3$.

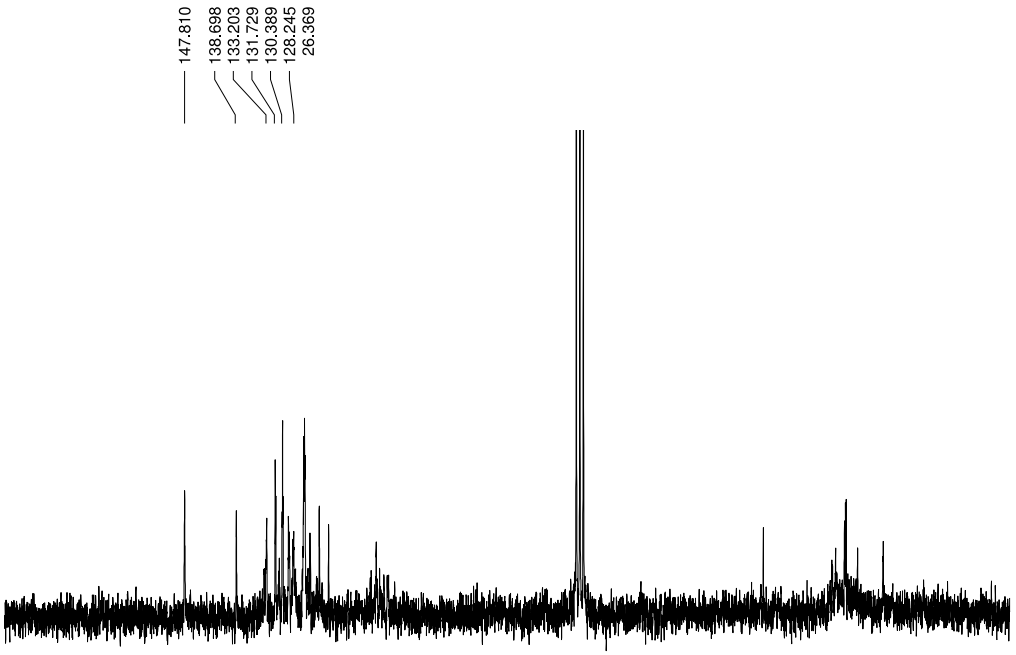


Figure S6. $^{13}$C NMR spectrum of **5** in $CDCl_3$.

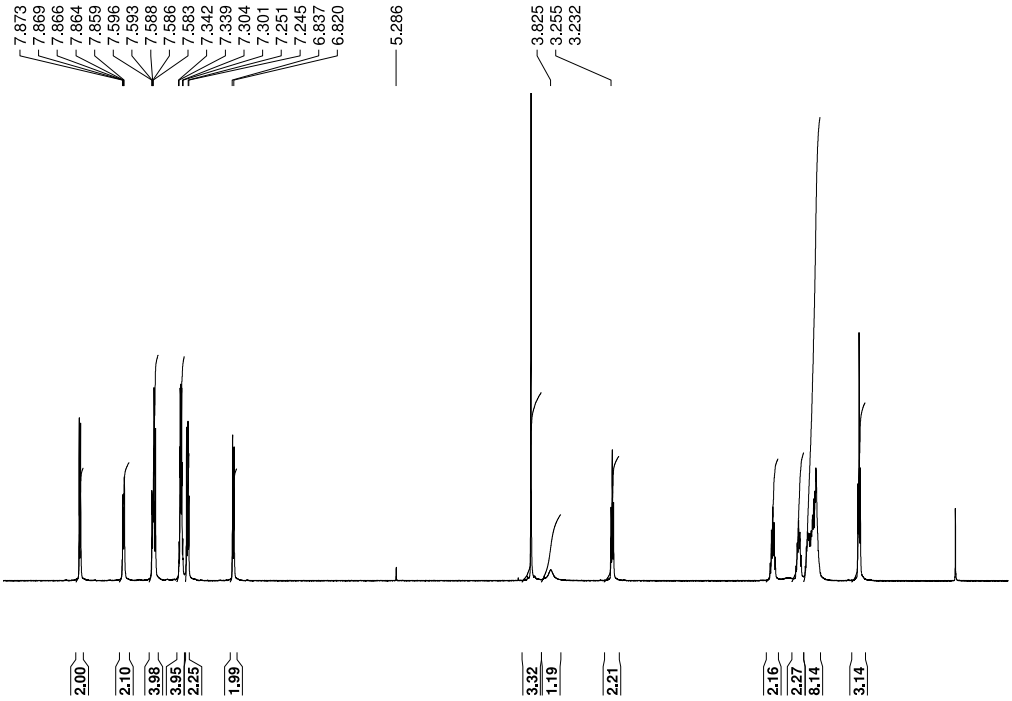


Figure S7. $^{1}$H NMR spectrum of **1** in $CDCl_3$.

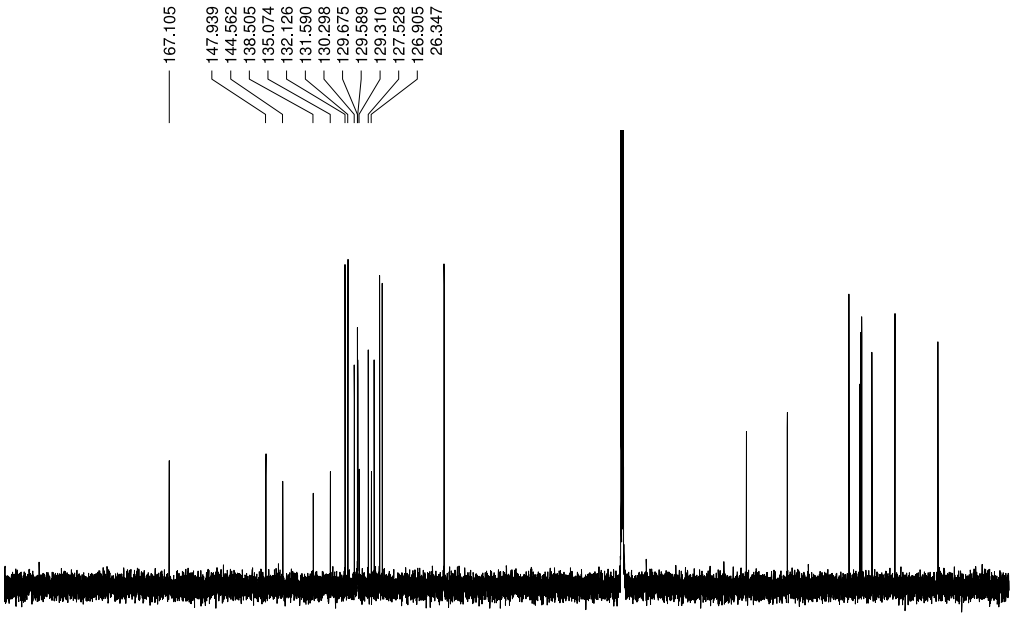


Figure S8. $^{13}$C NMR spectrum of **1** in $CDCl_3$.

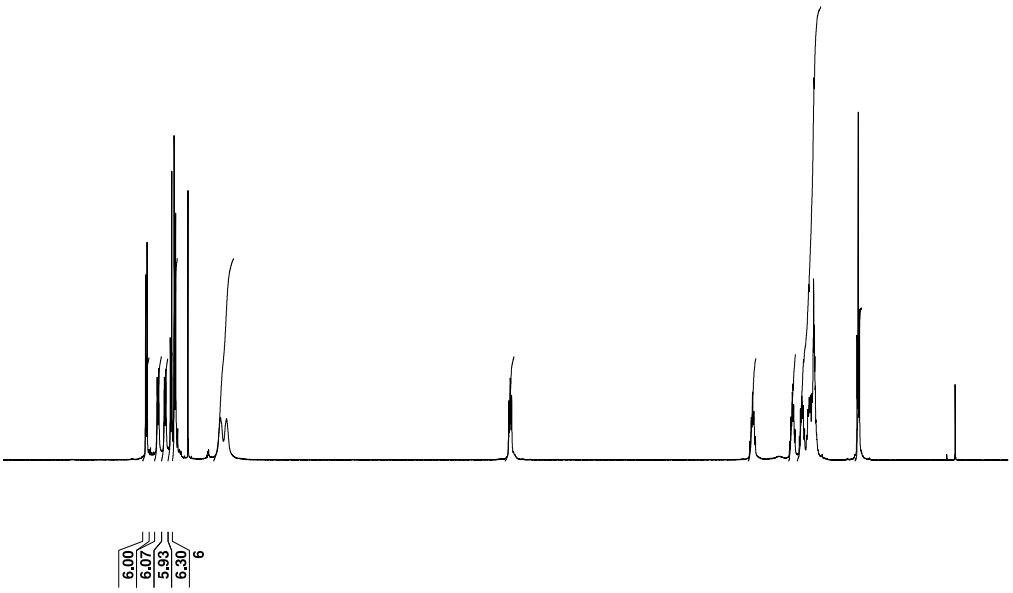


Figure S9. $^{1}$H NMR spectrum of **C3A** in $CDCl_3$.

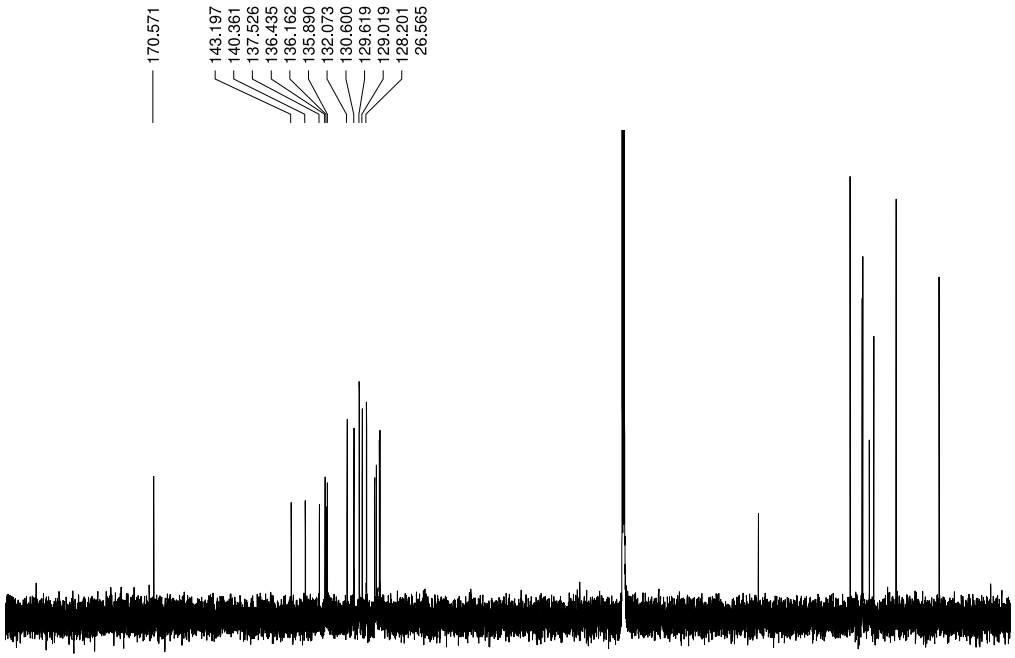


Figure S10. $^{13}$C NMR spectrum of **C3A** in $CDCl_3$.

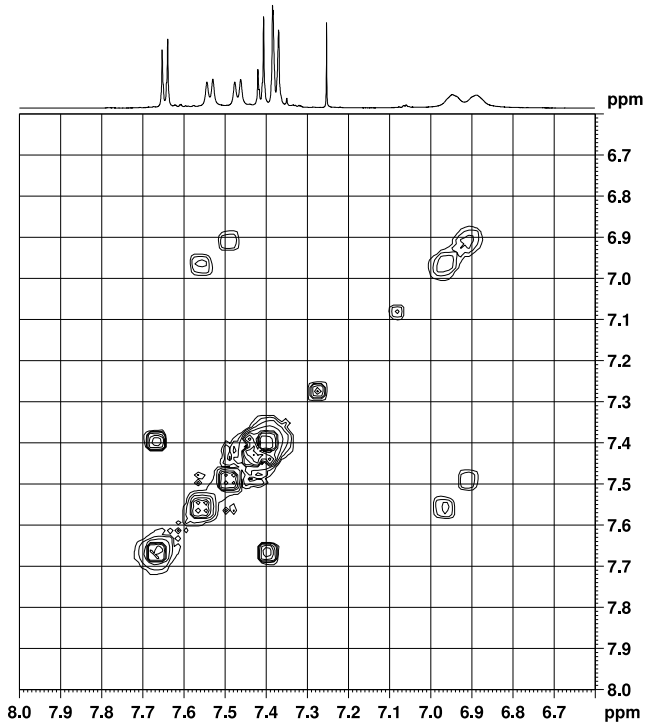


Figure S11. H-H COSY of **C3A** in $CDCl_3$ (aromatic region).

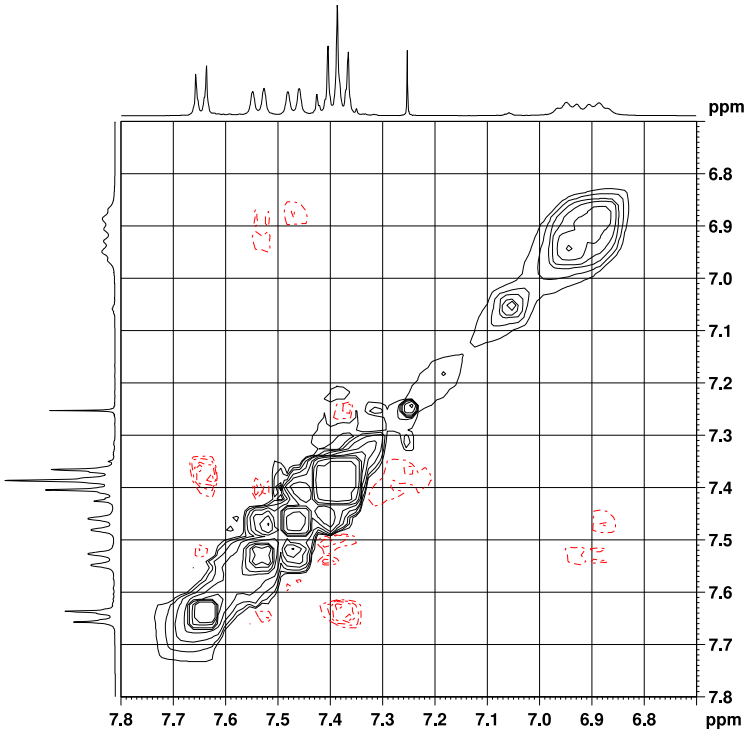


Figure S12. ROESY of **C3A** in $CDCl_3$ (aromatic region).

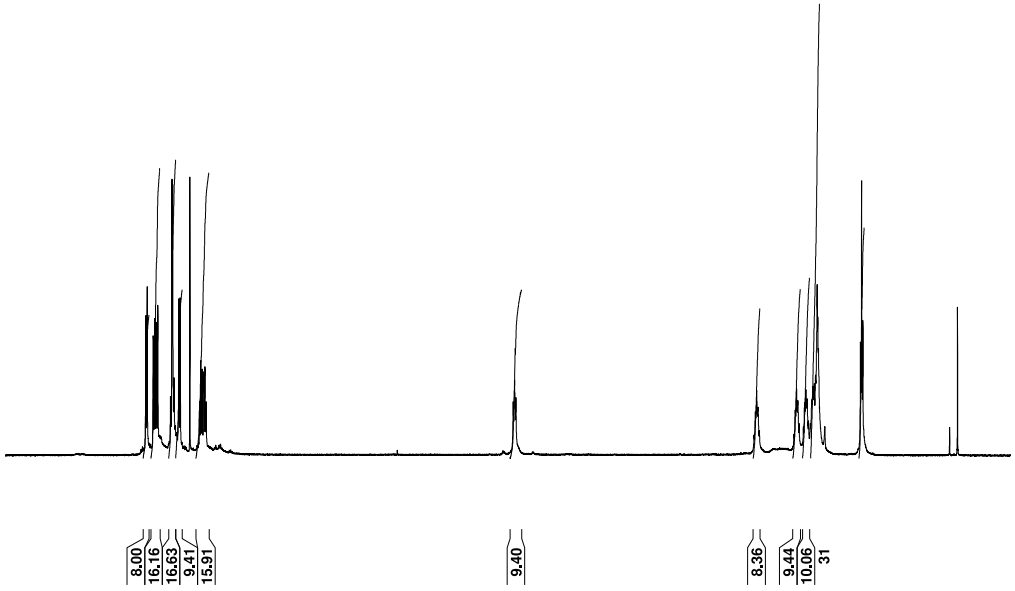


Figure S13. $^{1}$H NMR spectrum of **C4A** in $CDCl_3$.

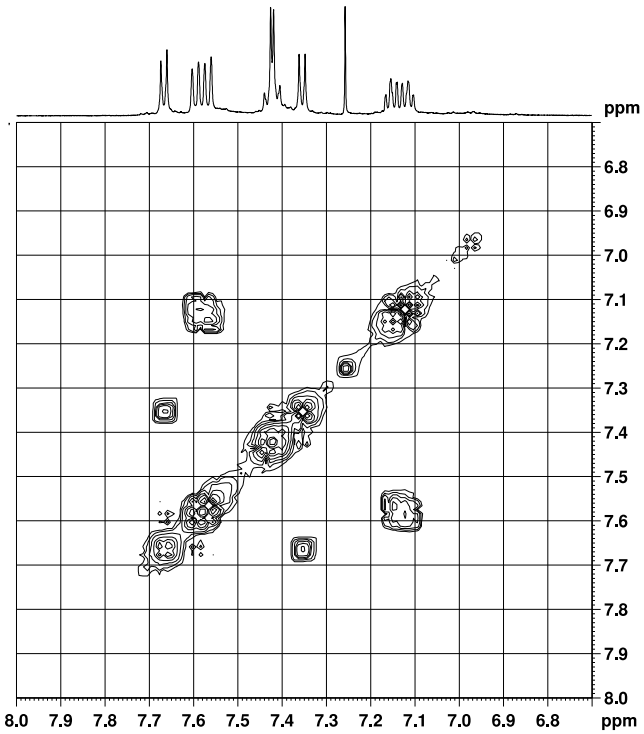


Figure S14. H-H COSY of **C4A** in $CDCl_3$ (aromatic region).

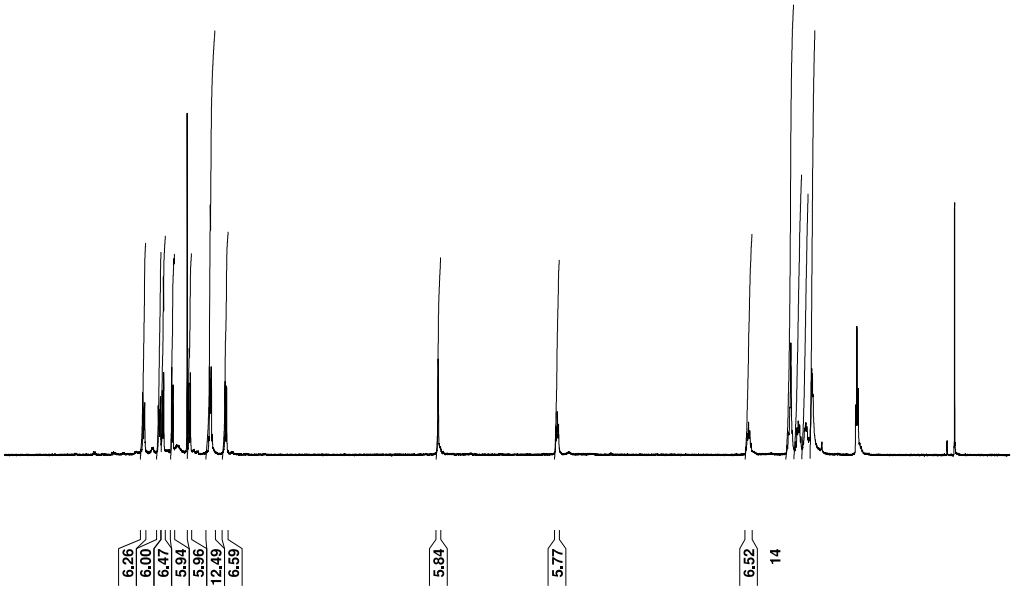


Figure S15. $^{1}$H NMR spectrum of **HC3A** in $CDCl_3$.

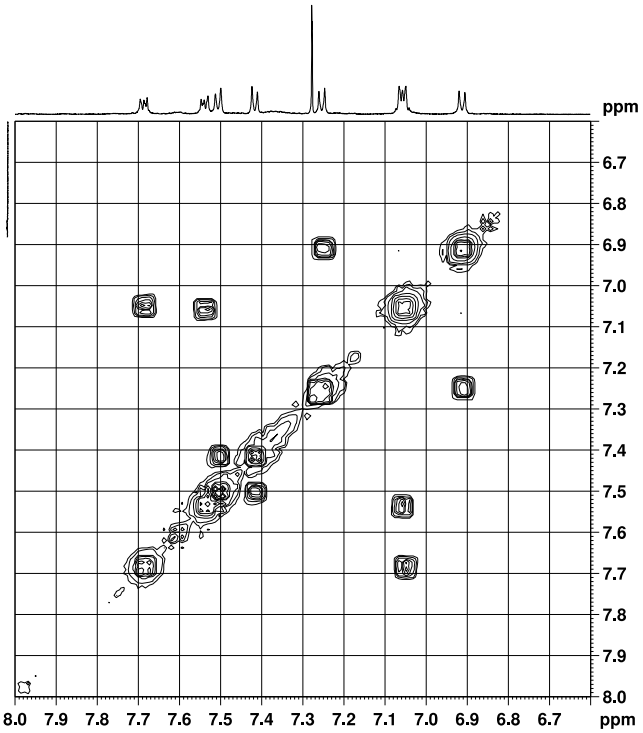


Figure S16. H-H COSY of **HC3A** in $CDCl_3$(aromatic region)

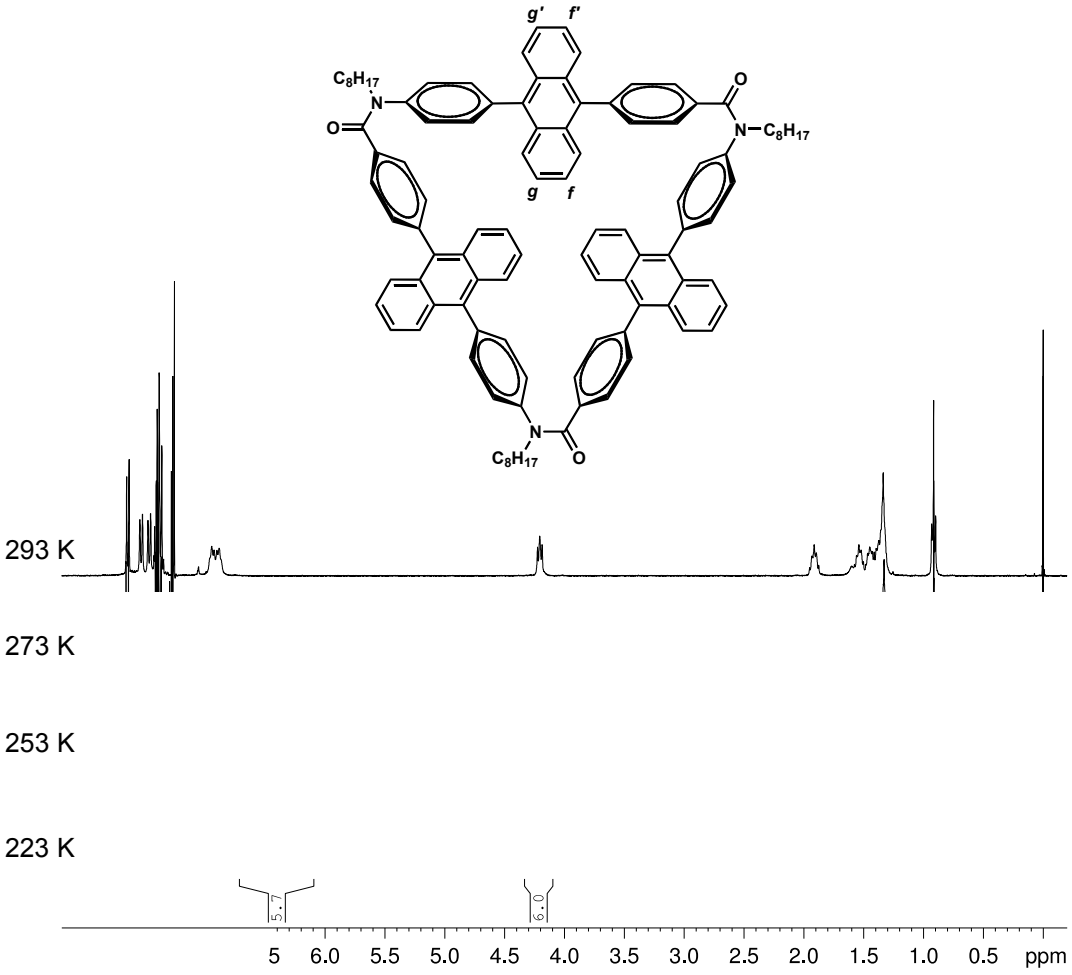


Figure S17. Variable-temperature $^{1}$H NMR spectra of **C3A** in $CDCl_3$.

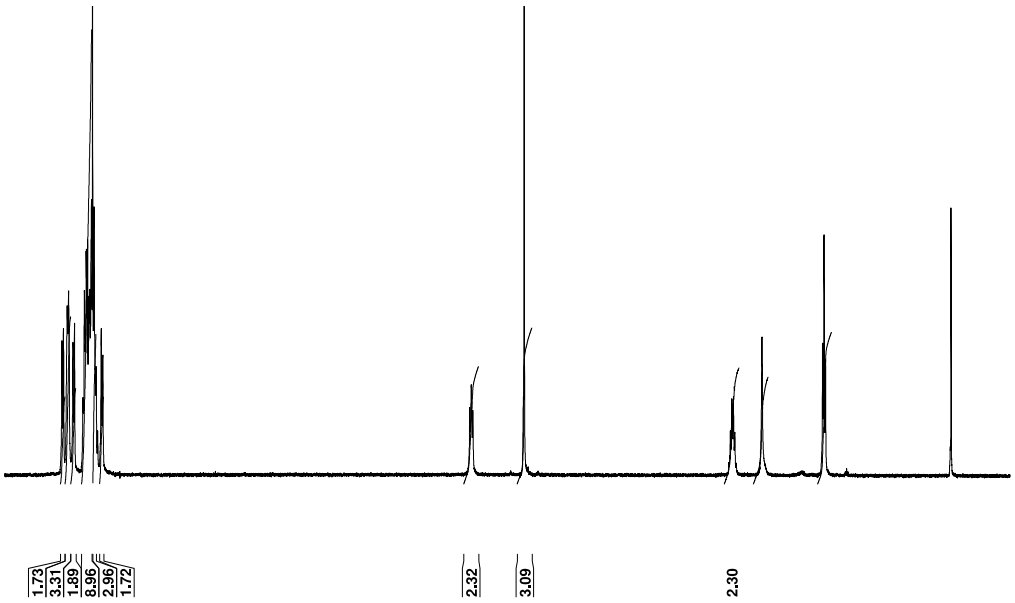


Figure S18. $^{1}$H NMR spectrum of **2** in $CDCl_3$.

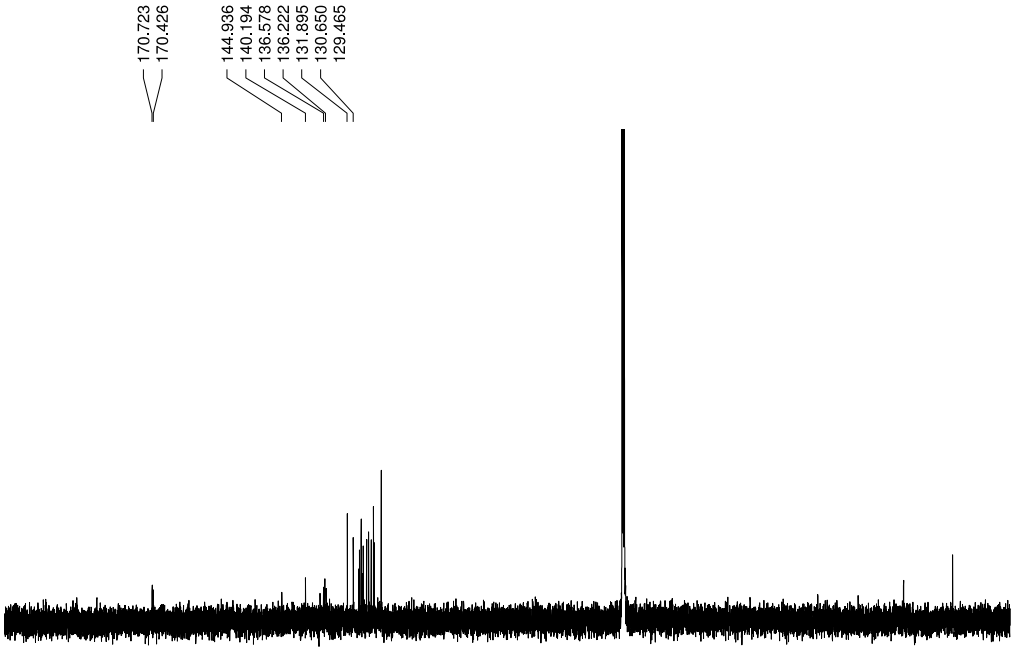


Figure S19. $^{13}$C NMR spectrum of **2** in $CDCl_3$.

2. GPC profiles

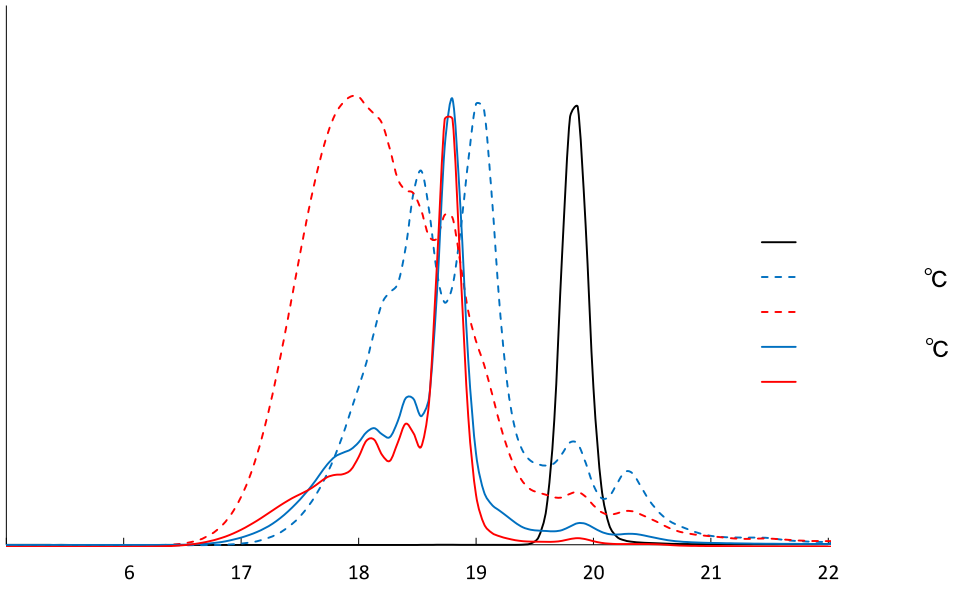


Figure S20. GPC (THF) profiles of reaction mixture.

3. MALDI-TOF MS

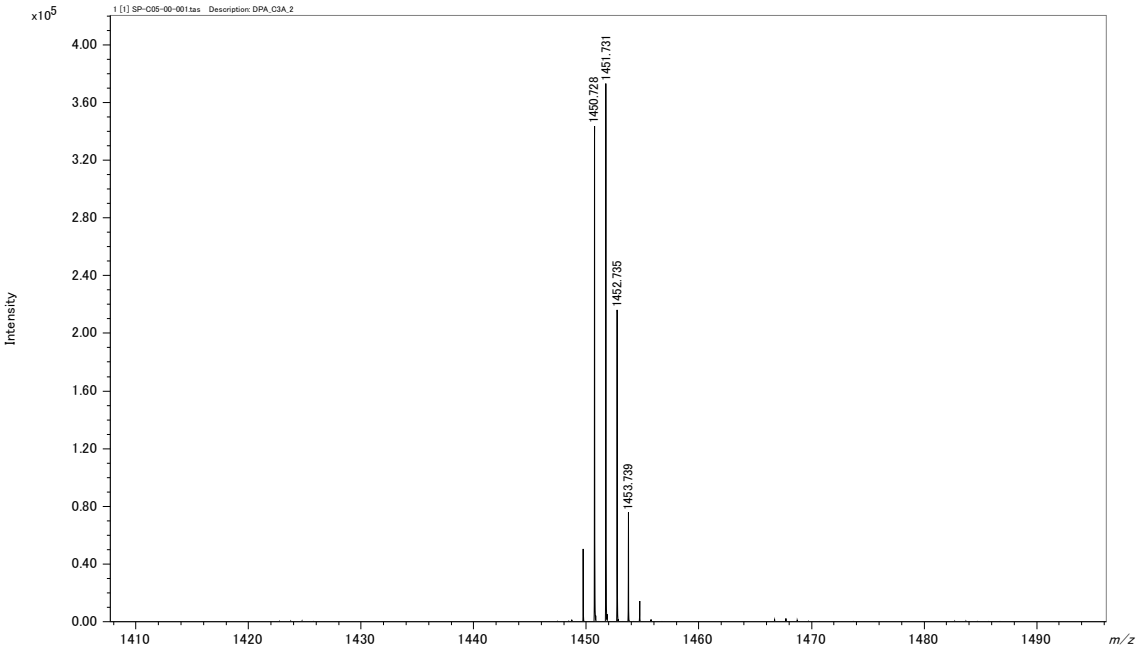


Figure S21. MALDI-TOF MS of **C3A**.

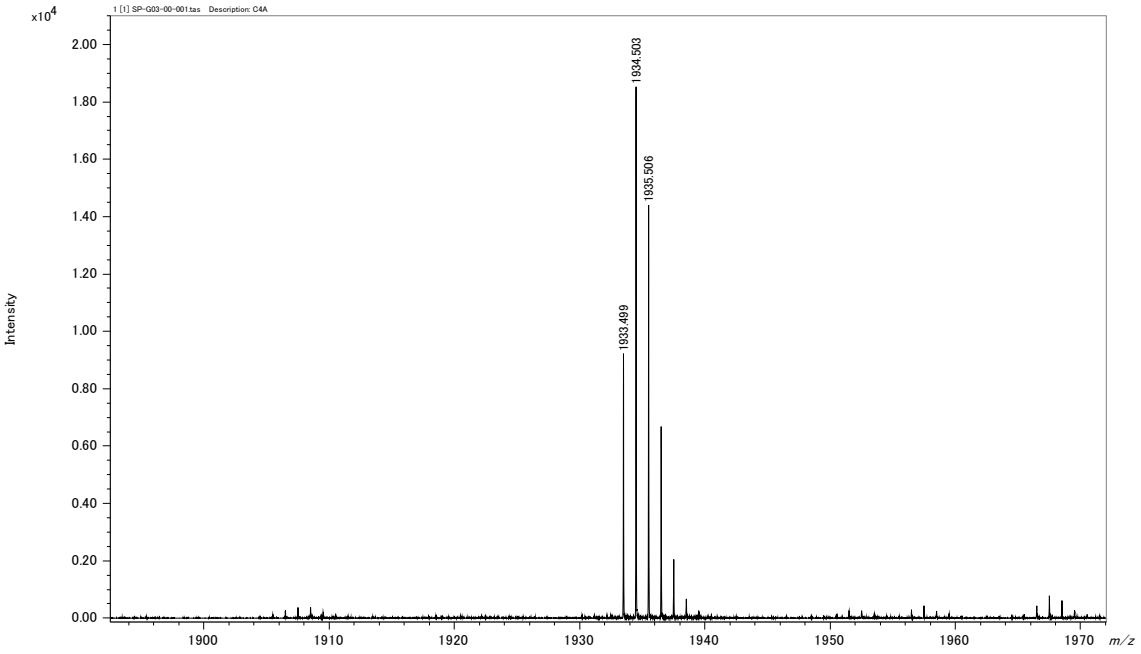


Figure S22. MALDI-TOF MS of **C4A**.

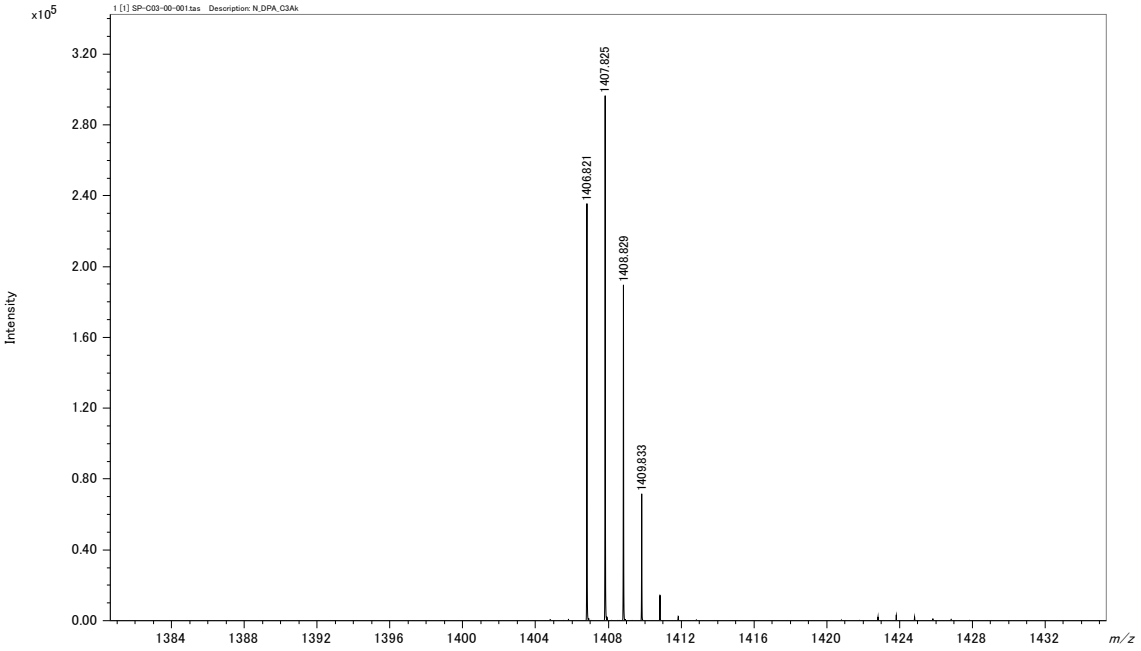


Figure S23. MALDI-TOF MS of **HC3A**.

4. UV and fluorescence spectra

Table S1. Detailed absorption and emission peak positions of **C3A** and **2** in DCM.

| Compound | $\lambda_{abs}$/nm | $\varepsilon$/$M^{-1}cm^{-1}$ | $\lambda_{em}$/nm | $\Phi^a$ |
|---|---|---|---|---|
| **C3A** | 377 | 52000 | 438 | 0.15 |
| **C4A** | 378 | 59900 | 439 | 0.06 |
| **2** | 376 | 14900 | 425 | 0.15 |

[a] Relative to quinine sulfate with $\Phi_{fl}$=0.55 as the standard.

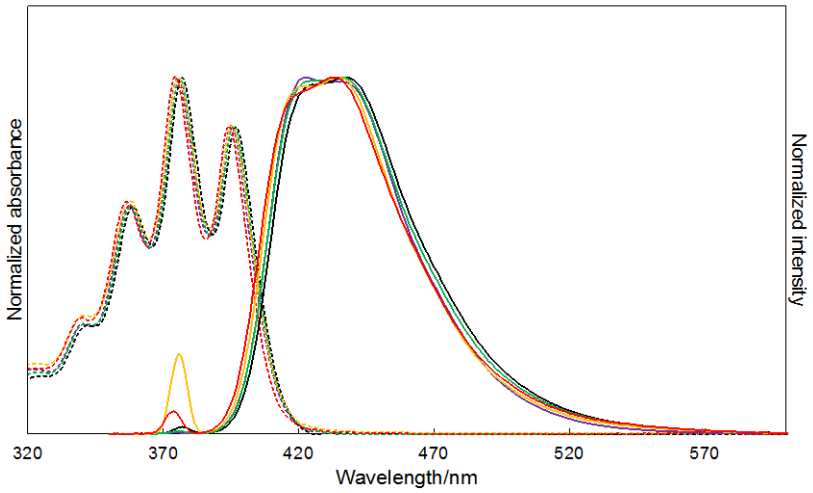


Figure S24. UV and fluorescence spectra of **C3A** in Cyclohexane (purple), THF (green), DCM (black), MeCN (orange), and MeOH (red) ($10^{-5}$ M).

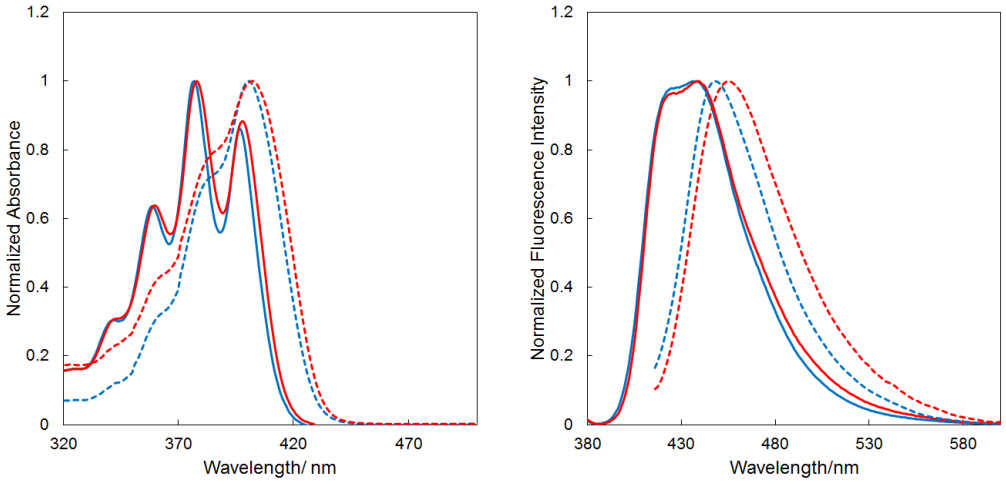


Figure S25. UV and fluorescence spectra of **C3A** (blue line) and **C4A** (red line) in DCM (solid line, $10^{-5}$M) and solid-state (dashed line).

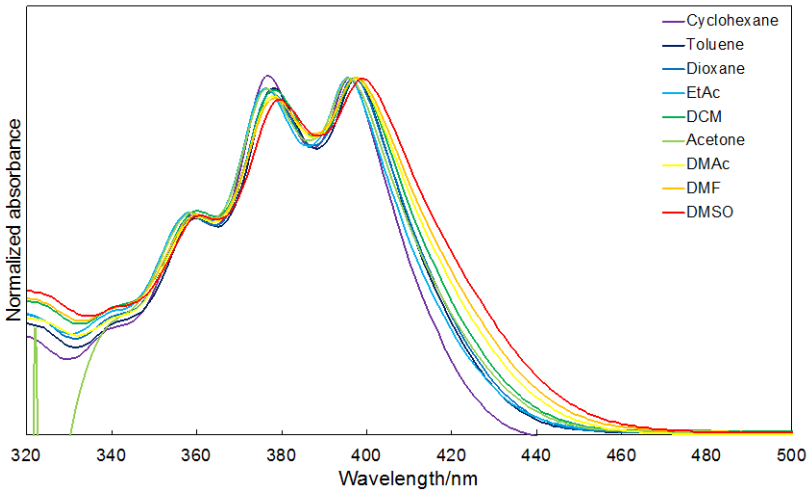


Figure S26. Solvent-dependent UV spectra of **HC3A** ($10^{-5}$ M).

Table S2. Detailed absorption and emission peak positions of **HC3A** in different solvents.

| | $E_T(30)$ /kcal·mol$^{-1}$ | **HC3A** | | | | |
|---|---|---|---|---|---|---|
| | | $\lambda_{abs}$ /nm | ε /M$^{-1}$cm$^{-1}$ | $\lambda_{em}$ /nm | Stokes shift /cm$^{-1}$ | Φ[a] /% |
| CH | 30.9 | 396 | 31000 | 449 | 2980.8 | 0.10 |
| Hexane | 31.0 | 395 | 27000 | 446 | 2894.9 | 0.10 |
| Toluene | 33.9 | 397 | 32500 | 464 | 3637.2 | 0.10 |
| DOX | 36.0 | 397 | 29200 | 472 | 4002.5 | 0.16 |
| EtOAc | 38.1 | 395 | 31700 | 488 | 4824.7 | 0.11 |
| DCM | 40.7 | 397 | 31300 | 489 | 4739.0 | 0.08 |
| Acetone | 42.2 | 396 | 31500 | 509 | 5606.2 | 0.09 |
| DMAc | 42.9 | 397 | 30500 | 525 | 6141.3 | 0.11 |
| DMF | 43.2 | 398 | 29400 | 527 | 6150.3 | 0.09 |
| DMSO | 45.1 | 399 | 23000 | 543 | 6646.5 | 0.10 |

[a] Relative to quinine sulfate with $\Phi_{fl}$=0.55 as the standard.

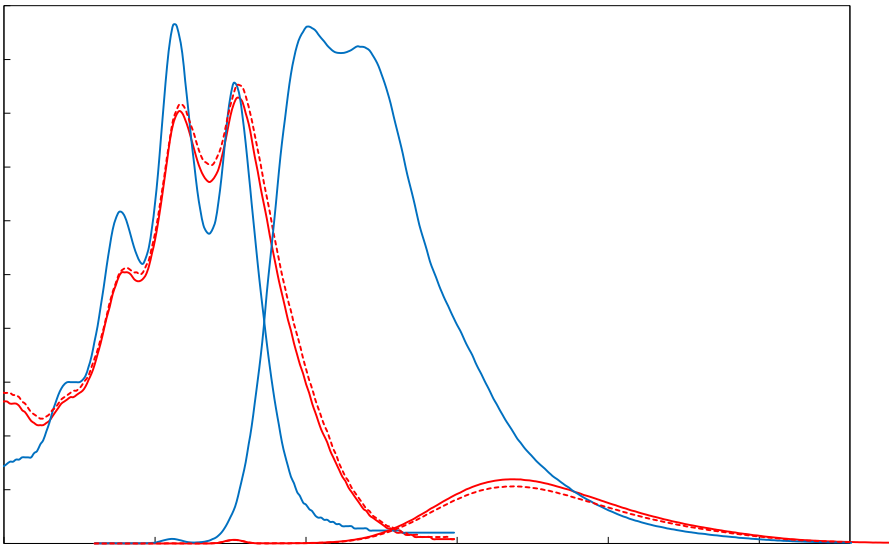

Figure S27. Changes in UV and fluorescence spectra of **HC3A** in DCM upon the addition of TFA and TEA; **HC3A** (red solid line), **HC3A**/TFA = 1/100 (blue solid line), and **HC3A**/TFA/TEA = 1/100/200 (red broken line).